DOI: 10.1007/s11099-018-0774-z PHOTOSYNTHETICA 56 (1): 342-353, 2018

Leptolyngbya CCM 4, a cyanobacterium with far-red photoacclimation from Cuatro Ciénegas Basin, México

C. GÓMEZ-LOJERO*,+, L. E. LEYVA-CASTILLO*, P. HERRERA-SALGADO*, J. BARRERA-ROJAS*, E. RÍOS-CASTRO** and E. B. GUTIÉRREZ-CIRLOS***

*Departmento de Bioquímica, Centro de Investigación y Estudios Avanzados del IPN, CdMx, Mexico**
*Laboratorio Nacional de Servicios Experimentales Centro de Investigación y Estudios Avanzados del IPN**,
*Unidad de Biomedicina, FES-Iztacala UNAM, Tlanepantla, Mexico****

Abstract

A cyanobacterium containing phycobiliproteins with far-red acclimation was isolated from Pozas Rojas, Cuatro Ciénegas, México. It was named *Leptolyngbya* CCM 4 after phylogenetic analysis and a description of its morphological characteristics. *Leptolyngbya* was grown in far-red light. Sucrose-gradient analysis of the pigments revealed two different colored bands of phycobiliproteins. A band at 60% sucrose was a phycocyanin containing phycobilisome; at 35% sucrose, a new type of phycobiliprotein absorbed at 710 nm. SDS-PAGE revealed the presence of two types of core-membrane linkers. Analysis of the hydrophobic pigments extracted from the thylakoid membranes revealed Chl *a, d*, and *f*. The ratio of Chl *f*/*a* was reversibly changed from 1:12–16 under far-red light to an undetectable concentration of Chl *f* under white light. Cuatro Ciénegas, a place surrounded by the desert, is a new ecosystem where a cyanobacterium, which grows in far-red light, was discovered.

Additional key words: chlorophyll *f*; Cuatro Ciénegas Basin; far-red light; photosynthesis; phycobilisomes.

Introduction

Phycobiliproteins (PBPs) are light-harvesting pigments in cyanobacteria, glaucophyta, and red algae. All organisms with PBPs synthesize allophycocyanin (AP) and phycocyanin (PC). These two pigments extend their absorbance between 600 and 660 nm. Many cyanobacteria contain phycoerythrins (PE), which absorb between 500 and 580 nm. The PBPs absorb light in the green hole left by Chl *a* (Chen and Blankenship 2011). Phycobilisomes (PBSs) are from simple rod-arrays structure (Hu *et al.* 1999, Chen *et al.* 2009) to supramolecular complexes of PBPs and linker proteins that harvest light energy, mainly for PSII and to a lesser extent to PSI (Liu *et al.* 2013). Most cyanobacteria have the enzyme ferredoxin-$NADP^+$ reductase as an associated protein (Schluchter and Bryant 1992, Gómez-Lojero *et al.* 2003). There are two types of PBS structures in cyanobacteria: bundle-shaped (Guglielmi *et al.* 1981, Mendoza-Hernández *et al.* 2010) and hemidiscoidal (Sidler 1994). There are two substructures in the PBS: the core and, irradiating from the core, the PBS-rods (Bryant *et al.* 1979). The core can be bicylindrical, tricylindrical or pentacylindrical. There are six rods in bicylindrical (Yamanaka *et al.* 1978) and tricylindrical cores (Bryant *et al.* 1979, Adir 2005), whereas there are up to eight rods in the pentacylindrical core of *Anabaena* (Sidler 1994, Chang *et al.* 2015). The core is organized by the multidomain core membrane linker (L_{CM}). The first domain of L_{CM} is a PBP, which is one of the terminal energy acceptors of that PBS (Lundell *et al.* 1981) and drains its energy to PSII. The second domain is a loop that is believed to anchor the PBS to the PSII. A third type of domain is a 190-amino-acids linker-homolog that repeats at least once and is known as a REP-domain. Between the REPs, there are arms that

Received 28 June 2017, *accepted* 5 December 2017, *published as online-first* 10 January 2018.
+Corresponding author; email: cgomez@cinvestav.mx
Abbreviations: AP – allophycocyanin; Car – carboxisomes; CCA – complementary chromatic acclimation; CNE – clear native electrophoresis; FaRLiP – far-red light photoacclimation; FNR – ferredoxin-$NADP^+$ reductase; Fr. – fractions; L_{CM} – core membrane linker; PBP – phycobiliprotein; PBS – phycobilisome; PC – phycocyanin; PMSF – phenylmethylsulfonyl fluoride; REP – repetitive sequence; RL – red light; Th – thylakoid membranes; WCE – whole cell extract; WL – white light.
Acknowledgments: This paper is dedicated to the memory of Dr. David W Krogmann: professor, colleague, and friend. CGL thanks Dr. Valeria Souza for the opportunity to be at Cuatro Ciénegas in May, 2012, where the mat sample was obtained. The authors wish to thank to Mr. Jorge Zarco Mendoza for his technical expertise, Dr. Laura Ongay and Biologist Ma. Guadalupe Codiz of the Unidad de Biología Molecular, Instituto de Fisiología Celular UNAM for DNA sequencing, and Mrs. Leticia Gómez-Sandoval for her secretarial assistance.

separate them (Houmard *et al.* 1990, Sidler 1994). The number of REP domains is two in L_{CM} for bicylindrical cores, with a molecular mass of approximately 75 kDa; three REPs in L_{CM} for tricylindrical cores, with a molecular mass of approximately 100 kDa, and four REPs in the L_{CM} for pentacylindrical core, with a mass of approximately 120 kDa. Each core cylinder is formed with four AP trimers. The composition of the basal cylinders is unique, as each allophycocyanin trimer is different: trimer 1: $(\alpha^{AP}\beta^{AP})_3.L_C$; trimer 2: $(\alpha^{AP}\beta^{AP})_2\ \alpha^{Lcm}\ \beta^{18.5}$; trimer 3: $(\alpha^{AP}\beta^{AP})_3$; and trimer 4: $(\alpha^{AP}\beta^{AP})_2\ (\alpha^{APB}\beta^{AP})$. L_C, "L_C" is a small core linker of approximately 8 kDa (Gómez-Lojero *et al.* 1997). The other basal cylinder is antiparallel, and the order of the trimers is 4, 3, 2, 1 (Anderson and Eiserling 1986). Trimer four is the other terminal energy acceptor of PBS that drains energy to PSI (Dong *et al.* 2009). There are two terminal energy acceptors in the core of PBS for each photosystem (Mimuro *et al.* 1986, Reuter and Wehrmeyer 1990). The rods can be constituted of only PC hexamers or of PC hexamers plus hexamers of PE or phycocyanoerythrin. Some phycoerythrin-producing cyanobacteria have complementary chromatic acclimation (CCA), which implies that the quantity of both PEs and PCs can be altered; however, the amount of AP remains constant (Tandeau de Marsac and Houmard 1988). CCA results from compositional remodeling of the rods and occurs through transcriptional regulation of specific PBPs and linker genes (Grossman 2003, Kehoe and Gutu 2006). The core and the first hexamer of the rods are always the same, independent of the light used to grow the cyanobacterium with CCA (Pérez-Gómez *et al.* 2012).

PBPs with components absorbing >700 nm were recently found in several cyanobacteria that are capable of far-red light photoacclimation, termed FaRLiP according to Gan and Bryant (2015). All PBPs described in FaRLiP are homologs of AP subunits. *Leptolyngbya* JSC-1 exhibits CCA and FaRLiP, which includes synthesis of Chl *d* and *f* and remodeling of not only PBS but also the core of both photosystems. A hemidiscoidal PBS with a pentacylindrical core was present in CCA and hemidiscoidal PBS with bicylindrical core is found when cells are grown in far-red light. In JSC-1, the substitution appears in all the core components of the PBSs, except the small linker L_C^8 and $\beta^{AP\ 18.5}$ (Gan *et al.* 2014a). A new PBS, which consists only a bicylindrical core, was reported in the filamentous cyanobacterium *Halomicronema hongdechloris*. The remodeling of PBS was a complete replacement of hemidiscoidal PBSs grown in white light with a small bicylindrical core-PBS grown in far-red light. This core-PBS has two absorbance peaks at 650 and 712 nm (Li *et al.* 2016). There is a third cyanobacterium, *Synechococcus* PCC 7335, in which the PBS of the FaRLiP have been characterized. *Synechococcus* produces bicylindrical cores that contain AP subunits paralogs. In *Synechococcus* sp. PCC 7335, there is no complete change of phycobilisomes, but rather a coexistence of the hemidiscoidal PBS with a tricylindrical core and a bicylindrical core-PBS (Ho *et al.* 2016a).

Chl *a* is the major pigment of the organisms that utilize oxygenic photosynthesis, such as cyanobacteria, algae, and plants. Chl *a* not only harvests the extremes of light in the visible region but is also the transducer at the reaction centers, transforming the light energy in charge separation in PSI (Jordan *et al.* 2001) and PSII (Umena *et al.* 2011). Only two Chls, divinyl-Chl *a* and Chl *d,* have been known to replace the function of Chl *a* as the antenna and as energy transducer (Chisholm *et al.* 1988, Mielke *et al.* 2013). The red peak in the absorption spectrum of divinyl Chl *a* is similar to Chl *a,* and the energy properties are the same. Chl *d* absorbs far-red light or near infrared 700–740 nm light and functions as a major pigment in the cyanobacterium *Acaryochloris marina* and related species (Loughlin *et al.* 2013). It has been shown that divinyl Chl *a* and Chl *d* function as energy transducers in the reaction center of PSI and PSII (Mielke *et al.* 2011). Recently a new Chl was reported and designated "*f* " (Chen *et al.* 2010). This Chl *f* absorbs at >700 nm, further in the red region than Chl *d*. Chl *f* has been found in at least 9 different cyanobacteria and in four of the five subsections of cyanobacteria. In the phylogenetic tree, the species described with Chl *f* are distant from each other and are from different habitats (Gan and Bryant 2015, Behrendt *et al.* 2015). In all cyanobacteria, in which the presence of Chl *f* has been reported, the major pigment is Chl *a* (Chen *et al.* 2012, Akutsu *et al.* 2011, Gan *et al.* 2014b). We report here the isolation of a filamentous cyanobacterium, *Leptolyngbya* CCM 4, from Cuatro Ciénegas Basin, México. CCM 4 was isolated from a mat with a multilayer of cyanobacteria that was below a layer of sand (Alcaraz *et al.* 2008, Souza *et al.* 2012). Characterization of the cyanobacterium was based on morphology, ultrastructure, 16S rDNA-based phylogeny, and analysis of the secondary structure of the D1-D1' helix of the 16S-23S internal transcribed spacer (ITS). We present data for two types of PBSs with their own pigments and linkers. The data show that this cyanobacterium presents far-red light photoacclimation, and we identified Chls *a, d*, and *f*. We also present initial data of the distribution of Chl *f* in enriched preparations of PSI and PSII.

Materials and methods

Isolation of *Leptolyngbya* CCM 4 and growth conditions: The cyanobacterium was obtained from a thick green mat from Humedales, Pozas Rojas, Cuatro Ciénegas Basin, México. The blue-green soil-mat was plated in a Petri dish on 1.5% agar in A^+ growth medium (Stevens *et al.* 1973) supplemented with vitamin B12 under white light lamps. Filaments were picked and transferred to 20 mL of liquid medium grown under far-red light using

halogen lamp (70 W) with blue and red filters during two weeks. The light intensity at the surface of the glass container was of 10 μmol(photon) m^{-2} s^{-1}. It was transferred to liquid medium of 50 mL in a flask of 250 mL and growth for two more weeks. The last transfer was to 1,800 mL of the same liquid medium with a magnetic stirrer and continuous flux of 5% CO_2 in air (V/V), during four weeks. The light intensities were measured with a *Quantitherm Hansatech* light meter (King's Lynn, UK).

Light and transmission electron microscopy: The cells were mounted on slides under glass coverslips. The cells were visualized using a (*Velab*) microscope with immersed 100 × objective and recorded with a digital camera.

The cells were fixed in 3% glutaraldehyde, 6% sucrose in PBS buffer overnight at 4°C, rinsed in PBS buffer, and then were post-fixed with 1% osmium tetroxide, stained in uranyl acetate for four min, and dehydrated in a graded series of ethanol from 50 to 100%, 10 min each step, and infiltrated with a resin. The samples were polymerized at 70°C for 60 h (Cárabez-Trejo and Sandoval 1974). Ultrathin sections were cut on the ultramicrotome using diamond knives (*E.I. Dupont*, Boston Ma, USA) collected on 300 mesh, pioloform coated on thin bar copper grids, and stained with saturated aqueous uranyl acetate for 30 min and by lead citrate for 4 min. All sections were visualized using a transmission electron microscope (*JEOL JEM 12000 EII*, Japan) at 80 kV images were captured using digital camera of 11 MP.

DNA isolation, PCR amplification and sequencing: Genomic DNA was purified using the method described for *Anabaena* sp. PCC 7120 (Curtis and Haselkorn 1983) obtained from one g (wet mass) of cultured cells of *Leptolyngbya* CCM 4, grown under white fluorescent light. The gene encoding 16S rDNA and the internally transcribed spacer (ITS) were amplified using a forward universal bacterial primer UB16S27-F (AGAGTTTGATCCTGGCTCAG), obtained from Taton *et al.* (2003). The reverse cyanobacterial primer CYA23S30-R (CTTCGCCTCTGTGTGCCTAGGT) was obtained from Couradeau *et al.* (2011). The 2nd forward cyanobacterial primer was designed from *Synechococcus* PCC 7002 gene encoding 16S rDNA in the present investigation (GGTAGCCGTACCGGAAGGTGTGGCTGGATC) and it was named CYA16S1428-F. The PCR product obtained using the primers UB16S27-F and CYA23S30-R, was close to 2,000 bp. The PCR of ITS (internal transcribed spacer) was obtained using the primers: CYA16S1428-F and the same reverse primer used before (CYA23S30-R). Two PCR products were obtained and named ITS-L (large) of 472 bp and ITS-S (short) of 344 nt.

Reactions were performed under the following conditions: 30 cycles of denaturation 94°C for 15 s, annealing at 52°C or 50°C for 60 s, and elongation at 72°C for 60 s at the end of the cycles a final incubation of 10 min at 72°C was allowed. The PCR products were sequenced and confirmed from two individual repeats of PCR reactions. The sequences were obtained by using the primers described above, at the Unidad de Biología Molecular of the Instituto de Fisiología Celular, UNAM. Sequence *BLAST* conducted us to find the closest cyanobacterium at NCBI.

Pigment extraction and HPLC analysis: Pigments were extracted from cells or membranes by following procedure: 1 mL of cells or membranes with eight volumes of methanol and one volume of acetone. The extract was filtered through *Whatman* paper and spin down with microfuge before the spectrum or the injection to the HPLC was done. The spectrum from 350–750 nm was recorded. Pigments were analyzed by HPLC on a 4 × 250 mm analytical *Spectrosil* C18 column (*Supelco*) using an *UltiMate 3000 Standard Dual System* (*Thermo Scientific Inc.*, USA). Data was acquired by diode array detector (*Waltham*, Ma, USA). Samples of 200 μL dissolved in 85% methanol and 10 mM of ammonium acetate (solvent A) were injected. Pigments were eluted from the column at flow rate of 1.5 mL min^{-1}. The solvent system and elution conditions were the following: solvent A was applied during 5 min; 5–12 min linear gradient to 6% of solvent A, 92% methanol and 2% acetone; 12–15 min linear gradient to 100% methanol; 15–18 min linear gradient 90% methanol, 10% acetone; 18–20 min, linear gradient 20% methanol, 80% acetone; 20–26 min, 20% methanol, 80% acetone; 26–35 min, linear gradient to 100% acetone (Moore *et al.* 1995).

Whole-cell extract (WCE) preparation: *Leptolyngbya* CCM 4 cells were harvested by filtration with *Nytal* nylon net (15-nm mesh) and grounded in a mortar. Approximately 14 g(wet mass) of CCM 4 were washed with 42 mL of 50 mM EDTA and 10% of NaCl at pH 8.0 (to free the cell filaments from the biofilm). The suspension was homogenized at full speed with a *Teflon* pestle and centrifuged 500 × *g* for 10 min. All the steps were carried out at room temperature and centrifugation at 22°C. All the solutions contained 1 mM of PMSF, 0.1% sodium azide, and 10 mM Na_2EDTA. The cells were washed again but this time with 0.85 M Na^+/K^+ phosphate buffer at pH 8.0. After centrifugation, the cells were weighted and suspended in a 1 to 10 relation with the phosphate buffer referred above. The suspension was homogenized again at full speed and put in a sonic bath for 30 min and centrifuged at 23,500 × *g* for 10 min. Whole cell extracts (WCE) were produced by disrupting cells by four successive passes through a French pressure cell operated at 18,000 psi. The broken cells were centrifuged for 10 min at 27,000 × *g* and the supernatant is the WCE.

Isolation of PBS by sucrose density gradient centrifugation: *Triton X-100* was added to the WCE to a concentration of 1.2% (v/v). The solution was stirred for 30 min at room temperature and then centrifuged for 30 min at 23,500 × *g* at 22°C (*Beckmann* rotor *JA-20*). The

sucrose step gradients consisted of 2, 5, 4, and 3 mL of 0.5, 0.75, 1.0, and 2.0 M sucrose solutions in 0.75 M Na^+/K^+ phosphate buffer pH 8.0. Samples of 4 mL, Triton-treated WCE were layered onto the sucrose gradient. The gradient was centrifuged at 185,000 × *g* for 3 h at 22°C (*Beckmann* rotor *70 Ti*). The gradients were collected from bottom to top in 1-mL aliquots. Absorption spectra of all Fr. were obtained by scanning from 350 to 750 nm.

Chl determination: The amount of Chl *a* and Chl *f* in cells was calculated according to equations described for methanol-extracted pigments (Li *et al.* 2014).

$$\text{Chl } a\ [\mu g\ mL^{-1}] = 12.52\ A_{665\text{-}750\ nm} - 2.28\ A_{707\text{-}750\ nm}$$
$$\text{Chl } f\ [\mu g\ mL^{-1}] = 12.78\ A_{707\text{-}750nm} - 0.07\ A_{665\text{-}750nm}$$

For acetone-extracted pigments, the amount of Chl was calculated according to the equations:

$$\text{Chl } f\ (mM) = A_{698\text{-}750\ nm}/77.97$$
$$\text{Chl } a\ (mM) = \{A_{665\text{-}750\ nm} - [\text{Chl } f]\ 13.3\}/78.36$$

It was based on the extinction coefficients published in Li *et al.* (2012).

Isolation of thylakoid membrane complexes by sucrose density gradient centrifugation: The same steps as for obtaining the WCE were followed, but the cells were washed with a buffer containing 0.05 M Tris, 10% NaCl at pH 8.0, with the inhibitors referred above. The cells were broken in the Tris buffer. All steps for membrane preparation were carried out at 4°C. The WCE was centrifuged at 148,000 × *g* during 20 min at 4°C. The membranes were suspended in a minimum volume and the Chl content was measured. The amount of Chl obtained was around 0.8 mg mL^{-1} and a solution of 20% DDM was added to a final concentration at 0.5%. The suspension was gently stirred during 30 min at 4°C. The solubilized membranes were centrifuged as before. From the supernatant, an aliquot was obtained and the Chl was measured. The solubilized sample was diluted with the same buffer with 0.5% of DDM to obtain 0.2 mg(Chl) mL^{-1} and loaded to a sucrose gradient. The sucrose step gradients consisted of 2, 3, 3, 2, 2, and 2.5 mL of 0.25, 0.5, 0.75, 1.0, 1.2, and 2.0 M sucrose solutions in the Tris buffer supplemented with 0.01% of DDM. The step gradient was centrifuged at 185,000 × *g* during 3 h at 4°C. The gradient aliquots were obtained as before. Absorption spectra were obtained as before.

Sample and acrylamide gel preparation for clear native electrophoresis (CNE): A sucrose gradient Fr. containing the green band of interest was pooled from two sucrose gradient tubes (two Fr. of 1 mL each), the sucrose concentration was measured (w/w) with an Abbe diffracting apparatus. The fast sedimentation green band (Fr. 6, 31% of sucrose) was diluted with 10 mL of the same buffer in which the membranes were solubilized. The sample was concentrated with an *Amicon* ultrafiltration cell with a *YM10* membrane in order to reduce the volume to 2 mL, and the sucrose concentration was measured again. The sample was further concentrated with a centricon ultracell *YM10 Millipore* to 0.5 mL. The Chl was measured and adjusted between 10–15 μg in 100 μL. Separating acrylamide 4–13% linear gradient gels were used for separation of DDM-solubilized thylakoid membrane complexes. Separating and condensation gels were cast at room temperature. After removal of the combs, the gels were overlaid with gel buffer and stored at 4°C for least 2 h prior to electrophoresis (Wittig *et al.* 2007). A maximum of 200 μl was applied per gel well.

SDS-PAGE for second dimension: The SDS-PAGE was performed as described by Schägger and von Jagow (1987) with the following adjustments: a 1.2-cm lane of the first dimension gel with the membrane complexes was excised, dipped into 10 mM of DTT, 2.5% of SDS in 62 mM Tris-HCl, pH 8, at 37°C during 2 h. The strip of the first dimension gel was placed on a glass plate at the position of the stacking gels. The second dimension gel was of 10% of acrylamide and the stacking gel of 4%. A well was included for molecular mass markers. The electrophoresis was started at 35 V × 3 h and the voltage was set to 95 V × 12 h (overnight) and finally 125 V for approximately 4 h.

SDS-PAGE and immunoblot of PBS: Electrophoresis was performed as previously described (Schägger and von Jagow 1987). Samples were diluted and precipitated with cold trichloroacetic acid to a final concentration of 15% (w/v). The pellet was suspended in digestion buffer and heated for 20 min at 60°C in a water bath. Samples were loaded onto 10% slab gel. A mixture of bovine serum albumin, ovalbumin, chymotrypsinogen, lysozyme, and horse heart cytochrome *c* (each 1 mg mL^{-1}), was used as molecular mass marker. The proteins in gels were stained with *Coomassie Brilliant Blue G-250* (*BioRad*, Hercules, CA). For immunoblotting, samples with FNR activity, equivalent of 54 nmol(DCPIP) min^{-1} were concentrated by precipitation**.** The proteins were transferred to Sequi-Blot PVDF membrane (*BioRad*, Hercules, CA) using a semi-dry system. A rabbit polyclonal primary antibodies against FNR, or against rod linker of 30 kDa or against core-membrane linker of *Arthrospira maxima* were raised in our laboratory, and an anti-rabbit horseradish peroxidase-coupled secondary antibody was used as previously described (Pérez-Gómez *et al.* 2012).

Results

Isolation of Chl *f* containing cyanobacterium: An oxygenic photosynthetic filamentous cyanobacteria containing Chl *f* was isolated from a microbial soil-mat covered with sand (Fig. 1*A*), from Pozas Rojas, Cuatro Ciénegas Basin, Mexico. Pozas Rojas is a fluctuating desiccation pond. The Cuatro Ciénegas Basin is surrounded by the desert of Chihuahua (Souza *et al.* 2008). From a preliminary analysis, we detected a PBP with absorption maximum at 710 nm, then we started to grow the cyanobacterium in far-red light (Gan *et al.* 2014a). We named this new cyanobacterium as CCM 4. Under the light microscope, CCM 4 corresponds to filamentous non-heterocyst cyanobacterium (Fig. 1*B*). Under transmission electron microscopy (Fig. 1*C*), the cells are cylinders of 0.8–1.2 μm diameter and with variable length in average of 2 μm. In the cytoplasm, four thylakoid membranes run in parallel to the longitudinal axis in each side of the cell. The polyhedral shape of the particles in the center of the cell and the electron dense appearance (Stanier 1988) can be used to identify them as carboxisomes (Car). The polyphosphate bodies appear as holes within the cells (Stanier 1988), presumably due to volatilization under the electron beam. The cells appear surrounded by a fibrous multilayered sheath with a thickness of 200 nm. The three typical layers in cyanobacteria, the cytoplasmic membrane (Cm), the peptidoglycan layer (Pg) and the outer membrane (Om) are observed (Fig. 1*D*). Also a terminal apical cell, triangle shape is shown (Fig. 1*E*).

Phylogenetic analysis: The following sequences were submited to GenBank: the 16S ribosomal RNA gene, partial sequence (1,452 bp); 16S-23S ribosomal RNA internal transcribed spacer (ITS_L 472 bp), tRNA-Ile, and tRNA-Ala genes, complete sequence; and 23S ribosomal RNA gene, partial sequence of *Leptolyngbya* CCM 4. [Accession number, GenBank: KY999936 (total submission: 1910 bp)]. By the NCBI, CCM 4 sequence against nucleotide-whole genome shotgun sequence *BLAST* search, 100 cyanobacterial sequences with an identity from 88 to 92% were aligned (Zhang *et al.* 2000). The 16S rDNA sequence of CCM 4 was analyzed for its taxonomic position using the 100 cyanobacterial sequences. Neighbor joining tree (Fig. 1S*A*, *supplement available online*) indicate that CCM 4 is in the cyanobacterial LPP group, together with *Halomicronema hongdechloris,* several *Leptolyngbya*, and in a cluster with *Leptolyngbya* sp. KIOST, *Nodosilinea nodulosa* PCC 7104, and *Phormidium tenue* NIES 30 (Fig. 1S*B*). The identity of 16S rDNA between CCM 4 and *H. hongdechloris* was 92%, with *N. nodulosa* 93%, and between *H. hongdechloris* and *N. nodulosa* 93%.

Two PCR products of internal transcribed spacer (ITS) were obtained from CCM 4: a large one (ITS_L) with 472 bp, containing genes encoding two tRNAs, for isoleucine (anticodon GAU) and for alanine (anticodon UGC) and short one (ITS_S) of 344 bp lacking the tRNAs.

We proceed to make the analysis of secondary structure of ITS_L motif D1-D1' helix of CCM 4 and other cyanobacteria present in the cluster in which CCM 4 appear in the phylogenetic tree (Fig. 2S, *supplement available online*). The D1-D1' helix was obtained using Mfold (Zuker 2003) folded at 22°C (RNA folding form version 2.3 energies). The D1-D1' helix of CCM 4 consisted of 62 nt with a 7 nt in the unilateral bulge with a

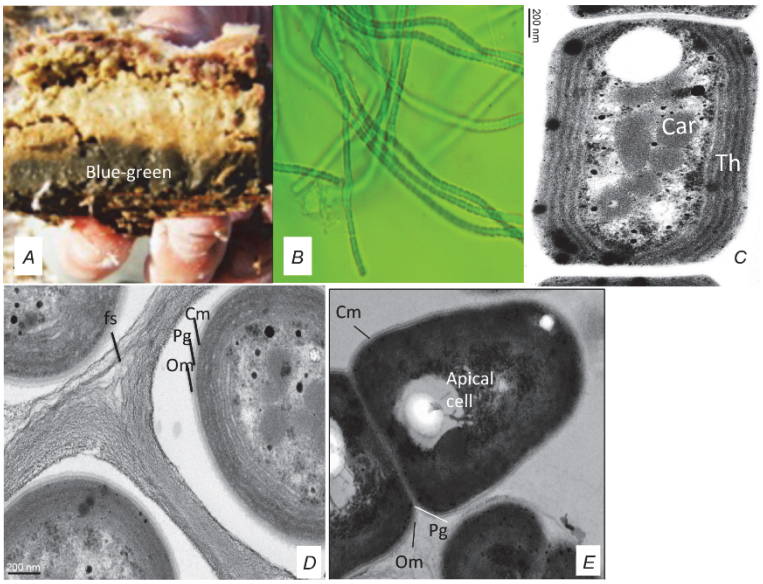

Fig. 1. Light microscopy and transmission electron microscopy images of CCM 4. (*A*) Cross section of the thick mat of Pozas rojas Cuatro Ciénegas from which CCM 4 was obtained (width of the nail 1.5 cm). (*B*) Light microscopy image of CCM 4 filamentous cells (100 ×). (*C–E*) Transmission electron micrographs of ultrathin section of CCM 4 cells: (*C*) longitudinal section of a CCM 4 cell (scale bar of 200 nm), the cytoplasm is surrounded by several thylakoid membranes (Th), in the center of the cytoplasm, several carboxysomes are visible (Car). (*D*) Cross-section [scale bar of 200 nm] showing multilayered fibril sheath (fs), outer membrane (Om), peptidoglycan layer (Pg), and cytoplasmic membrane (Cm). (*E*) Apical cell.

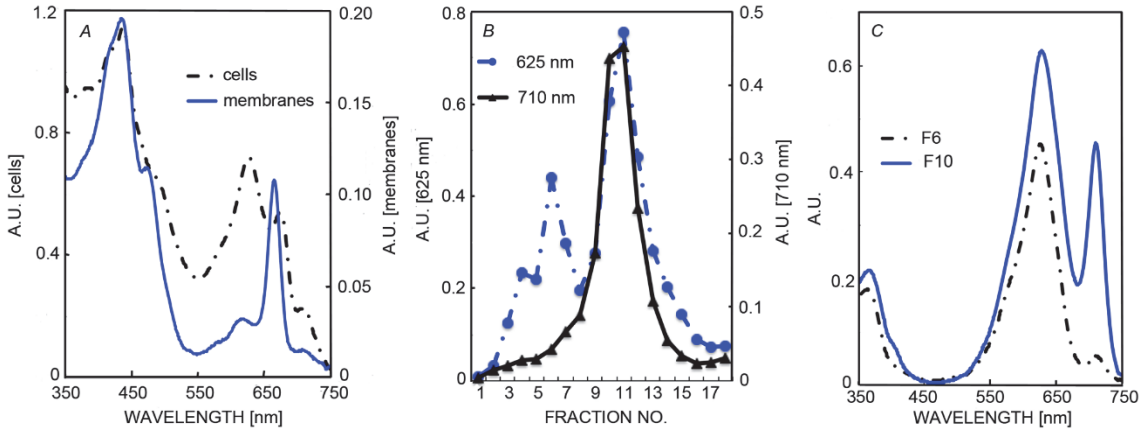

Fig. 2. Pigment analysis of CCM 4 at room temperature. (*A*) Absorption spectra of whole cell extract (*discontinuous line*) and methanol extract of the WCE (*solid line*). (*B*) The pattern of Fr. (*bottom to top*) obtained from a sucrose gradient of the WCE solubilized by *Triton X-100*. The absorbance of each Fr. at 650 nm (*filled circles*) for AP and 710 nm (*filled triangles*) for a new phycobiliprotein are indicated. (*C*) Absorption spectra of Fr. 6 (*discontinuous line*), Fr. 10 (*solid line*).

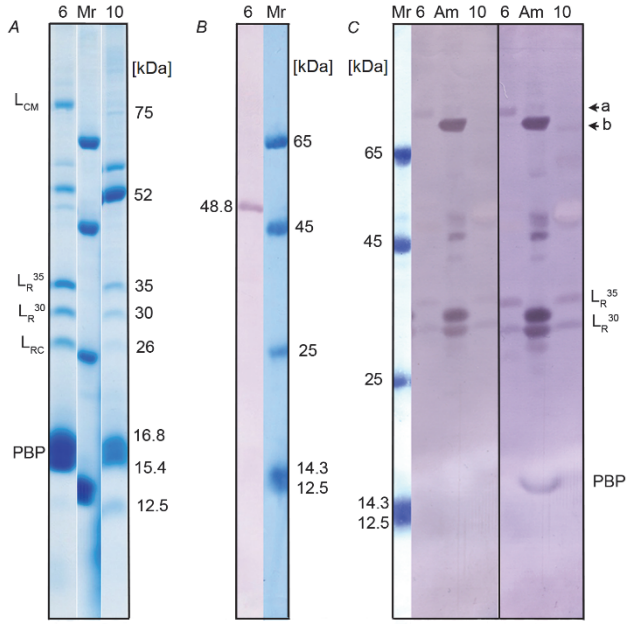

Fig. 3. SDS-PAGE and immunoblot analysis of Fr. 6 and 10 of the sucrose gradient. (*A*) *Coomassie Blue*-stained 10–20 % acrylamide gel (1.5 mm thick) containing the resolved bands of Fr. 6 and Fr. 10. (*B*) Immunoblot analysis of Fr. 6 of the sucrose gradient, The PVDF membrane was probed with an *Arthrospira maxima* FNR antibody. (*C*) Immunoblot analysis of Fr. 6 and 10 probed with two *A. maxima* antibodies. Left lanes probed with an *A. maxima* 30 kDa rod-linker (L_R) antibody, right lanes probed with *A. maxima* core membrane-linker (L_{CM}) antibody. Lanes marked with number 6 are from Fr. 6, lanes marked with Am are PBSs from *A. maxima* (control). Lanes marked with number 10 correspond to Fr. 10. Mr: molecular mass markers. Arrows a and b are L_{CM} of hemidiscoidal-PBS and core-PBS, respectively.

sequence CAAACCU. The loop at the end of the helix (10 nt) is followed by an apex of 5 nt, the loop is subtended by a helix and contains a CUCC-GGAG stem with canonical pairing. The primary central helix has two opposed small bulges (Fig. 2S). The genus *Nodosilinea* was proposed for a cyanobacteria that has the capacity to form nodules under low-light illumination and a characteristic secondary structure of D1-D1' helix (Perkerson *et al.* 2011). Basically, the characteristics of D1-D1' helix, which species of the genus *Nodosilinea* share, are the bulge of 6 nt with the sequence CACUCU and that apex loop is subtended by helix which contains a GAA-UUA stem (unusual for non-canonical G:A pairing). None of them are present in the D1-D1' of CCM 4 even though the general shape is similar. The difference with *Halomicronema hongdechloris* is conspicuous, too (Fig. 2S). In conclusion, we decided to name our CCM 4 cyanobacterium as a *Leptolyngbya* CCM 4, although the genus is non-monophyletic.

Hydrosoluble pigments in *Leptolyngbya* CCM 4 cells grown in far-red light: The WCE spectrum (Fig. 2*A,* dotted line) of CCM 4 showed four peaks at 438 nm, 620, 678, and a new peak at 720 nm, and one shoulder at 490 nm. The absorption peaks correspond to the blue green cyanobacteria pigments Chl *a*, PC, and the shoulder to carotenes. The peak at 720 nm corresponds to new pigments recently described in cyanobacteria that have FaRLiP. In the spectrum of pigment extracted with methanol from the WCE (Fig. 2*A,* continuous line), besides the peaks of the Chl *a* and shoulder of the carotenes, there is a small absorption peak, now observed at 707 nm presumably corresponding to Chl *f*.

Fig. 2*B* shows the distribution of PBPs after sucrose gradient centrifugation of the WCE treated with *Triton X-100*. Two profiles are presented: the 650 nm absorbance profile, representative of AP (circles), shows three main peaks corresponding to Fr. 4, 6, and 10. The sedimenting peak 4 and 6 contained the PBS, the 30% of the total absorption of allophycocyanin was in this Fr. (1–7). The spectrum of Fr. 6, is shown in Fig. 2*C*, from which 1 to 2.13 absorbance ratio of AP:PC ($A.U._{650nm}$:$A.U._{625nm}$)

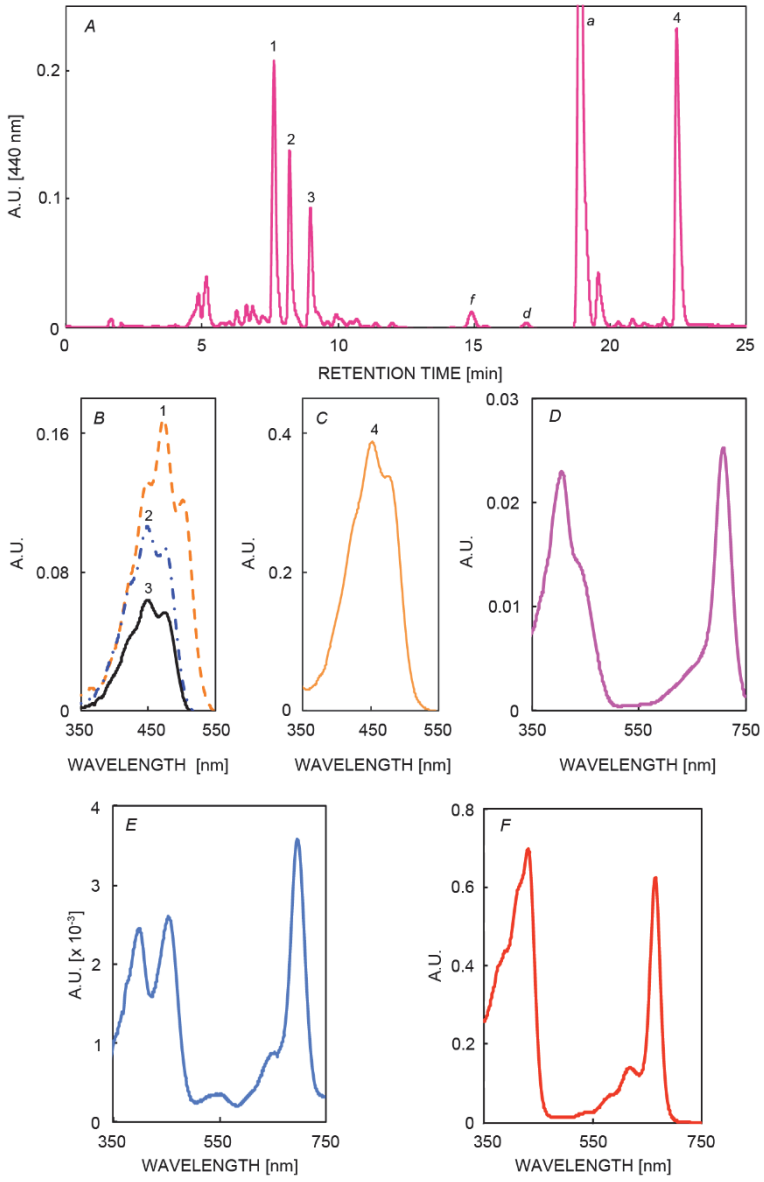

Fig. 4. Liposoluble pigments separation by HPLC and their absorption spectra. (*A*) HPLC retention profile of pigments extracted from cells with methanol, monitored at 440 nm. (*B*) Absorption spectra of carotenoids. (*C*) Absorption spectrum of β-carotene. (*D*) Absorption spectrum of Chl *f*. (*E*) Absorption spectrum of Chl *d*. (*F*) Absorption spectrum of Chl *a*.

obtained for the PBS. The slow migrating peak represented 70% of the absorption of allophycocyanin (Fr. 7–13). The 710-nm absorbance profile (Fig. 2*B,* triangles) shows that slow peak contained the enriched PBP induced by the far-red light. The spectrum of Fr. 10 (continuous line) is shown in Fig. 2*C*. The absorbance ratio $A.U._{.625nm}$: $A.U._{.711nm}$ of Fr. 10 was 1:0.626 and for Fr. 6 was 1:0.1. The Fr. 6 and 10 were assayed for sucrose concentration, the obtained values were: 31% and 22.4% w/w of sucrose, respectively.

The phycobilisome components: Fig. 3 and Fig. 4S (*supplement available online*) show the SDS-PAGE and the immunoblot analysis of Fr. 6 and 10 of the sucrose centrifugation gradient. Lanes 6 from Fig. 3*A* and Fig. 4S*A* together with the spectrum of Fig. 2*C* (discontinuous line) show the typical components of the hemidiscoidal PBS with PC rods: the core membrane linker L_{CM}, the rod linkers L_R^{35}, L_R^{30}, and the rod-core linker, L_{RC}^{26}. In addition, the mass of the PBPs has a range from 17.5 to 15.2 kDa for PC and AP subunits. The immunoblot of Fig. 3*B*, probed with the antibody against the FNR of *A. maxima*, shows the presence of FNR as an associated enzyme of the hemidiscoidal PBS in Fr. 6, in which diaphorase activity was also detected. The apparent molecular mass of 48.8 kDa corresponds to the three-domain enzyme, FNR-3D (Alcántara-Sánchez *et al.* 2017). Lanes 10 of Fig. 3*A* and Fig. 4S*A* together with the absorption spectrum of Fig. 2*C* (solid line) show components attributable to the far-red induced PBS, a core-PBS, which migrates as the slow peak in the sucrose gradient. The predicted mass of the core membrane linker, L_{CM} of the core-PBS, is approximately 75 kDa in other cyanobacteria (Gan *et al.* 2014a, Li *et al.* 2016, Ho *et al.*

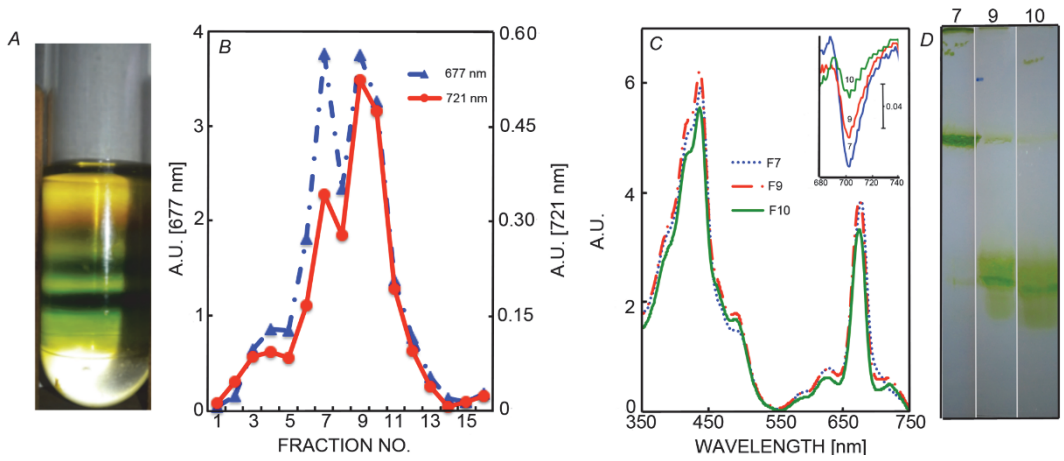

Fig. 5. Characterization of photosynthetic complexes obtained by sucrose gradient centrifugation of DDM-solubilized thylakoid membranes. (*A*) Sucrose density gradient in the centrifuge tube. (*B*) The pattern of Fr. (bottom to top) obtained from the sucrose gradient. The absorbance of each Fr. at 677 nm (*triangles*) and 720 nm (*circles*) are indicated. (*C*) Absorption spectra of Fr. 7, 9, and 10 and in the insert the light bleach of P_{700} of the same Fr. (*D*) CNE of the green Fr. 7, 9, and 10 from the sucrose gradient.

2017). Both gels show the components of the hemidiscoidal PBS but they are better defined in lane 6 of Fig. 3*A*, and the core PBS components are better resolved in Fig. 4S*A*. The immunoblots (Fig. 3*C* and Fig. 4S*B*) show the relative position of core-membrane linkers of the hemidiscoidal PBS (Fr. 6) and core-PBS (Fr. 10) relative to the core membrane linker of *Arthrospira maxima* (Am) whose PBSs have been characterized previously (Gómez-Lojero *et al.* 1997). Two arrows (a) and (b) show the positive bands obtained for Fr. 6 and 10, respectively. Arrow (a) is above the positive band of lane Am, ApcE of *A. maxima.* Arrow (b) is below of the core-membrane of *A. maxima*. Because of this difference in masses, we suggest that Fr. 6, has an hemidiscoidal-PBS containing a polypeptide of three REPs characteristic of a tricylindrical PBS core (Sidler 1994). In contrast, ApcE2 of the FaRLiP, core-PBS was lighter (Fr. 10), and we propose that this core-membrane linker is of two REPs characteristic of a bicylindrical core, as it was proposed for core-PBS induced under far-red light (Gan *et al.* 2014a, Li *et al.* 2016, Ho *et al.* 2016a). This core-PBS co-migrates in the sucrose gradient with Rubisco aggregates and rod substructures of PC with rod linkers, which can be seen in lane 10 of the electrophoretogram shown in Fig. 3*A* and Fig. 4S (marked with apparent mass of 52, 35, and 30 kDa).

The presence of Chl *f* in the thylakoid membrane: Pigment composition of the thylakoid membrane of CCM 4 were resolved by HPLC of the methanol–acetone extract (Fig. 4*A*). Fig. 4*B–C* revealed four carotenes and three Chls (Fig. 4*D–F*). Chl *a* was the more abundant pigment (Fig. 4*F*), with a maximal red peak at 662 nm, and its Soret peak at 438 nm. On average we found 20-times less of Chl *f* (Fig. 4*D*) than Chl *a* based on the absorbance maxima in the red and far-red of each Chl, which is close to 16 in methanol and 17.4 in acetone, concentration ratios obtained for [Chl *a*]/[Chl *f*] in CCM 4 cells. The far-red peak was at 704 nm and the Soret peak at 402 nm. The third Chl detected was Chl *d* (Fig. 4*E*) with maximum absorbance at 694 nm and the Soret band is split in two peaks at 395 nm and 450 nm. The Chl *d* was 200 times lower than Chl *a*. In addition to β-carotene (Fig. 4*C*), which is the more abundant carotene, there were other three carotenoids present in cyanobacteria (Fig. 4*B*).

Distribution of Chl *f* in the photosystems: The solubilization of the thylakoid membrane of CCM 4 with the mild detergent DDM and its separation in sucrose gradient centrifugation resulted in two green bands (Fig. 5*A*). Fig. 5*B* shows, the sedimentation profile of sucrose gradient, which was loaded with the supernatant of detergent-solubilized thylakoid membrane of CCM 4. The absorption profiles at 677 nm and 721 nm show two peaks corresponding to Fr. 7, 9, and 10. The most rapidly sedimenting Fr. contained PSI trimer with a ratio of absorbancies ($A.U._{677–750nm}/A.U._{721–750nm}$) of 11. The second peak in Fr. 9–10 contained a mixture of PSI and PSII with ratios of absorbancies at the same wavelengths ($A.U._{677–750nm}/A.U._{721–750\,nm}$) of 7 and 6.6, respectively. Fig. 5*C* shows the spectra of Fr. 7, 9, and 10, the spectra showing a shoulder for Fr. 7 and 9 and a well-defined peak in the far red for Fr. 10. In the insert, the difference spectra of P_{700}, [reduced (by ascorbate) – oxidized (with actinic light)] of the same Fr. (7, 9, and 10) are shown. The ratios $A.U._{677–750nm}/A.U._{701–725nm}$ for Fr. 7 was 150, for Fr. 9 was 220, and for Fr. 10 was 300, confirming that Fr. 7 contained most of the PSI. We only detected P_{700}. The CNE in Fig. 5*D* shows a single band in Fr. 7 and a complex mixture of at least three bands in Fr. 9 and 10.

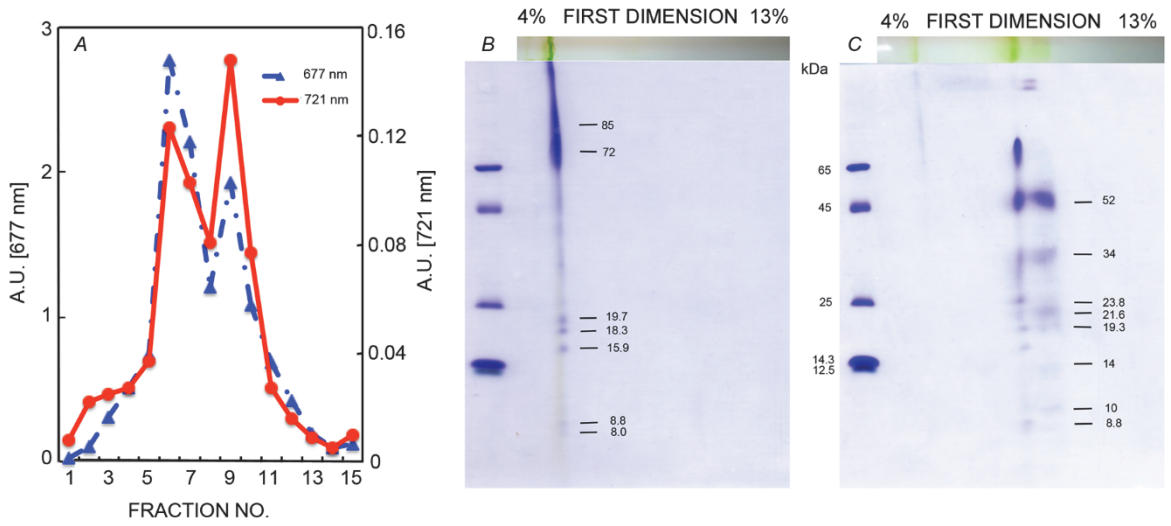

Fig. 6. Two-dimensional resolution of the green complexes from CCM 4. (*A*) The pattern of Fr. from the sucrose gradient. The absorbance at 677 nm (*triangles*) and 720 nm (*circles*) are indicated. (*B*) Two dimensional resolution of Fr. 6 of the sucrose gradient in *A*. First dimension: CN-PAGE of Fr. 6 of the sucrose gradient in *A* (horizontal strip). Second dimension: denaturing Tricine–SDS-PAGE, for resolution of the complex I of the first dimension into their individual protein subunits. (*C*) Two dimensional resolution of Fr. 9 of the sucrose gradient in *A*. The first dimension is a clear native PAGE of Fr. 9 (horizontal strip). Second dimension is a denaturing Tricine–SDS-PAGE for resolution of the splitted bands of the first dimension.

The components of the pigmented complexes: CNE separates protein complexes by their size and allows to isolate larger membrane supercomplexes and complexes, such as PSI trimer, PSI monomer, PSII dimer, PSII monomer, and PBS substructures. In Fr. 6 (Fig. 6*A*), only one green band was present (shown on top of Fig. 6*B*). A strip of the first dimension was subjected to a 2D SDS-PAGE. The *Coomassie blue*-stained, two-dimensional CN/SDS-PAGE gels are shown in Fig. 6*B–C*. We identified the PSI by their characteristic polypeptide pattern in Fig. 6*B*, the core proteins (PsaA and PsaB) of molecular masses of around 83 kDa, the three subunits of masses around 20 kDa (PsaL 18.1 kDa, PsaF of 17.8 kDa, and the PsaD of 15.1 kDa), and the small subunits below 10 kDa (PsaK of 9.6 kDa, PsaC of 8.8 kDa, and PsaE of 7.8 kDa) that were better resolved after silver staining, shown in Fig. 5S (*supplement available online*). In the CNE of Fr. 9, there was a split in two green bands, shown in the upper part of Fig. 6*C* and solved in the second dimension. The components of both green bands were solved in the second dimension seen in the same Fig. 6*C*. The thin band contained a mixture of subunits of both photosystems, and the widest band, but less intense in green, had very well distinguished protein components of the PSII. The PSII was identified by their characteristic molecular mass components: the proximal antennae CP 47 and CP 43 with masses approximately 50 kDa (PsbB, 56.3 kDa; PsbC, 51.6 kDa), the core subunits with apparent masses around 33 kDa (PsbA, 39.7 kDa, and PsbD, 39.2 kDa), the cluster of subunits around 20 kDa, and the small proteins below 10 kDa.

Discussion

Morphological and ultrastructure characterization: An oxygenic photosynthetic prokaryote isolated from a deep blue-green zone, CCM 4, was identified as a filamentous cyanobacterium with non-heterocyst cells, non-nodules as in the genus *Nodosilinea* has nodules (Perkerson 2011), and *Halomicronema* thinner cells than CCM 4 (Chen 2012), *see* Fig. 1. The thylakoid membranes are parallel at the long axis of the cells, which almost disappear at the septa region (Fig. 1*C*). The array of the thylakoid membranes is different than those in *Halomicronema hongdechloris* and *Nodosilinea rehakova*, which are at the periphery of the cells (Perkerson 2011, Chen 2012). The morphological and ultrastructural observations suggest that CCM 4 belongs to subsection III, *Oscillatoriales* of the *Cyanobacteria* (Castenholz *et al.* 2001).

Phylogenetical analysis: The values of identity (<93%) with *H. hongdechloris, Nodosilinea nodulosa* PCC 7104, *Phormidium tenue, Leptolyngbya* KIOST, and *Leptolyngbya* PCC 7375 (Fig. 1S*B*) placed the CCM 4 as a new species (Stackebrandt 1994). *Leptolyngbya* has been known as polyphyletic (Castenholtz *et al.* 2001), but new genera have been slowly recognized. *Halomicronema* (Chen *et al.* 2002) and *Nodosilinea* (Perkerson *et al.* 2011) are new genera, which were clustered with CCM 4 (Fig. 1S*B*). This clustering of CCM 4 in the LPP group brought us to discard or accept this genus for CCM 4. The secondary structure of D1-D1'helix of the 16S-23S ITS region has been suggested as a character useful for taxonomy analysis for *Nodosilinea* (Perkerson *et al.* 2011). We compared D1-D1' structures from several cyano-

bacteria, which were close, in 16S rDNA sequence data and are shown in Fig. 2S. We discarded the genus *Nodosilinea* since the conserved sequence (CACUCU) of the unilateral bulge was absent in CCM 4 and the noncanonical G-A pairing of the helix subtended the apex loop was also absent in CCM 4. We discarded the genus *Halomicronema* due to the presence of a loop at the apex of 8 nt in CCM 4 that is absent in the genus *Halomicronema* (Fig. 2S, *supplement available online*). In conclusion, by the morphological characterization and the phylogenetic analysis, we designated the genus *Leptolyngbya,* (*sensu lato*) for CCM 4 a nov. sp.

PBSs components: The hemidiscoidal-PBSs (Glazer 1989), isolated from cells of CCM 4 grown in far-red light, have an absorption peak at 625 nm and a shoulder at 650 nm corresponding to PC and AP (Fig. 2*C*). In addition, with the identified linkers (Fig. 3*A*, lane 6, and Fig. S4*A*, lane 6) we came to a definition of hemidiscoidal PBS with a tricylindrical core by the presence of L_{CM}, with three REPs, six rods with three PC hexamers by the presence of two rod linkers, L_R^{35} and L_R^{30}, one rod core linker (L_{RC}^{26}) and the associated FNR (Fig. 3*B*). The remodeling of the PBS in the FaRLiP consists of the appearance of pigments with absorption maximum at 711 nm (Fig. 2C) and a bicylindrical core (L_{CM}, with two REPs; Fig. 3*A*, lane 10, and 3*C*, lane 10; Fig. 4S*A*, lane 10, and 4*B*, lane 10). The PBP domain of this linker has the phycocyanobilin not attached covalently, since the cysteine is absent (Gan *et al.* 2014a, Ho *et al.* 2016a, Li *et al.* 2016). The usual way to identify the rod core membrane linker is by mass spectrometry (knowing the sequence of the L_{CM} protein, which is not the case) or Zn-inducing fluorescence staining (if the pigment remains attached to the protein in the gel after SDS denaturalization, which is not the case). We chose an antibody against the core-membrane linker (also the REPs domain maintains great similarity with the rod linkers). The size of the core membrane linker of the hemidiscoidal PBS (Fig. 3*A*, L_{CM} of lane 6; and lanes 6 of Fig. 2*C*, upper arrow) is heavier than that of *A. maxima* (Am) L_{CM}. The core membrane linker of the far-red PBS (lane 10 Fig. 3*A* and lanes 10 in Fig. 3*C*) is lighter than that of *A. maxima* L_{CM} (Am).

Membrane pigment composition: According to the retention time (Fig. 4*A*) and visible absorption spectra, we identified the Chl *f, d,* and *a* (Fig. 4*D–F*) in CCM 4. Chl *a* is the major Chl produced, followed by Chl *f* and very low amount of Chl *d.* Four carotenoids were observed in the pigment extracts (Fig. 4*B–C*); the most abundant was β-carotene (Fig. 4*C*). CCM 4 is the 7th reported strain, containing Chl *f* and Chl *d* (Airs *et al.* 2014, Gan *et al.* 2014b, 2015). Other three species produce only Chl *f*: *H. hongdechloris* (Chen *et al.* 2012), the unicellular cyanobacterium strain KC1 (Itoh *et al.* 2015), and a cavernous cyanobacterium (Behrendt *et al.* 2015). It remains to be clarified if Chl *d* is a byproduct of Chl *f* synthase, recently described (Ho *et al.* 2016b), or if there is a Chl *d* synthase.

Chl *f* in PSI and PSII produced under far-red light in CCM 4: In CCM 4, there is a coexistence of hemidiscoidal PBS with core-PBS in the FaRLiP. The remodeling of PBSs in the FaRLiP has been shown to be different between *H. hongdechloris*, JSC-1, and PCC 7335; in the first cyanobacterium, there is a substitution of the hemidiscoidal PBS by core-PBS (Li *et al.* 2016). In JSC-1, there is a substitution of hemidiscoidal pentacylindrical PBS by hemidiscoidal bicylindrical PBS (Gan *et al.* 2014a). In PCC 7335 and now CCM 4, there is a coexistence of the hemidiscoidal-PBS and the core-PBS (Ho *et al.* 2017). The question now arises about composition of the other two photosynthetic membrane complexes PSI and PSII: Is there a coexistence or this is 100% remodeling of the core of both photosystems? Both types of paralogs can be expected. The answer demands the use of mass spectrometry to identify the paralogs. We are in the process of obtaining these information and we started to separate the photosystems by sucrose gradient centrifugation and CNE (Fig. 5). The individual photosystems were identified by their characteristic polypeptides pattern in the two-dimensional resolution PAGE in Fig. 6 and the paralogs of both photosystems remain to be identified by mass spectrometry. The sequencing of the genome has been completed by MOgene (*St Louis*, MO USA) and we are in the process of genome annotation. Soon, we will have the answer if it is a partial or a complete photoacclimation of the CCM 4 photosystems.

Conclusion and perspectives: The results reported here show that *Leptolyngbya* CCM 4 can perform FaRLiP and thereby grows continuously in far-red light. CCM 4 produces Chls *a, f*, and *d* and phycobiliprotein paralogs absorbing at 710 nm. CCM 4 cells grown under red or white light produce PC-PBS (Fig. 3S). When CCM 4 is grown in far-red light, two types of PBS are produced: the hemidiscoidal PC-PBS and a core-PBS with PBP absorbing light at 710 nm with a L_{CM} with an apparent mass of 75 kDa that predicts a bicylindrical core. This strain, CCM 4, isolated from a sandy soil of Cuatro Ciénegas Basin, increases the diversity of environments where FaRLiP cyanobacteria have been detected. Multiple species of cyanobacteria, which are distant phylogenetically from each other, present FaRLiP. To explain the existence of FaRLiP in the five subsections of cyanobacteria, horizontal gene transfer has been proposed (Gan *et al.* 2014b). It remains to find out how frequent this can be in the dense mats of Cuatro Ciénegas Basin.

Further investigation remains to be done by exploring vertically, on a millimeter scale, the Cuatro Ciénegas mats. The differential depth penetration of light wavelengths in mats creates stratification of phototrophs adapted to the use of particular wavelengths of light. Four filtered light

zones can be defined in the mat where we can map the biological diversity. These four zones are from top to bottom: the Chl *a, b*, and phycocyanin zone, in which the blue orange and red light is absorbed, phycoerythrin zone in the green hole left by Chls, the Chl *d* and *f* zone in the far-red light, and finally in the deep zone (bacteriochlorophyll zone) in which light of >750 nm penetrates, the near-infrared light. This stratification of light penetration makes the microbial mats hot spots of bacterial diversity and constitutes a rich reservoir of genes and allows bacterial evolution by HGT. In addition to biological organisms causing filtration of light in Cuatro Ciénegas Basin, the sandy soil could select the far-red light (Gan *et al.* 2014b).

References

Adir N.: Elucidation of the molecular structures of components of the phycobilisome: Reconstructing a giant. – Photosynth. Res. **85**: 15-32, 2005.

Airs R.L., Temperton B., Sambles C. *et al*.: Chl *f* and Chl *d* are produced in the cyanobacterium *Chlorogloeopsis fritschii* when cultured under natural light and near-infrared radiation. – FEBS Lett. **588**: 3770-3777, 2014.

Akutsu S., Fujinuma D., Furukawa H. *et al*.: Pigment analysis of a Chl *f*-containing cyanobacterium strain KC1 isolated from Lake Biwa. – Photomed. Photobiol. **33**: 35-40, 2011.

Alcántara-Sánchez F., Leyva-Castillo L.E., Chagolla-López A. *et al.*: Distribution of isoforms of ferredoxin-NADP$^+$ reductase (FNR) in cyanobacteria in two growth conditions. – Int. J. Biochem. Cell B. **85**: 123-134, 2017.

Alcaraz L.D., Olmedo G., Bonilla G.: The genome of *Bacillus cohauilensis* reveals adaptations essential for survival in the relic of an ancient marine environment. – P. Natl. Acad. Sci. USA **105**: 5803-5808, 2008.

Anderson L., Eiserling F.A.: Asymmetrical core structure in phycobilisomes of the cyanobacterium *Synechocystis* sp. PCC 6701. – J. Mol. Biol. **191**: 441-451, 1986.

Behrendt L., Brejnrod A., Schliep M. *et al*.: Chl *f*-driven photosynthesis in a cavernous cyanobacterium. – ISME J. **9**: 2108-2111, 2015.

Bryant D.A., Guglielmi G., de Marsac N.T. *et al*.: The structure of the cyanobacterial phycobilisomes: a model. – Arch. Microbiol. **123**: 113-127, 1979.

Cárabez-Trejo A., Sandoval F.: A mitochondrial inner membrane preparation that sediments at 100 g. – J. Cell Biol. **62**: 877-881, 1974.

Castenholtz R.W., Rippka R., Herdman M., Wilmotte A.: Form-genus V. *Leptolyngbya* Anagnostidis and Komarek 1988. – In: Boone D.R., Castenholtz R.W. (ed.): Bergey's Manual of Systematic Bacteriology, Vol. 1. Pp. 544-546. Springer-Verlag, New York 2001.

Chang L., Liu X., Li Y. *et al*.: Structural organization of an intact phycobilisome and its association with photosystem II. – Cell Res. **25**: 726-737, 2015.

Chen M., Schliep M., Willows R.D. *et al*.: A red-shifted chlorophyl. – Science **329**: 1318-1319, 2010.

Chen M., Blankenship R.E.: Expanding the solar spectrum used by photosynthesis. – Trends Plant Sci **16**: 427-431, 2011.

Chen M., Li Y., Birch D., Willows R.D.: A cyanobacterium that contains Chl far red absorbing photopigment. – FEBS Lett. **586**: 3249-3254, 2012.

Chen M., Floetenmeyer M., Bibby T.S.: Supramolecular organization of phycobiliproteins in the chlorophyll *d*-containing cyanobacterium *Acariochloris marina.* – FEBS Lett. **583**: 2535-2539, 2009.

Chisholm S.W., Olson R.J., Zettler E.R. *et al*.: A novel free living prochlorophyte abundant in the oceanic euphotic zone. – Nature **334**: 340-343, 1988.

Couradeau E., Benzerara K., Moreira D. *et al*.: Prokaryotic and Eucaryotic communite structure in field and cultured microbialites from alkaline Lake Alchichica (Mexico). – PLoS ONE **6**: e28767, 2011.

Curtis S.E., Haselkorn R.: Isolation and sequence of the gene for large subunit of ribulose-1,5-bisphosphate carboxylase from the cyanobacterium *Anabaena* 7120. – P. Natl. Acad. Sci. USA **80**: 1835-1839, 1983.

Dong C., Tang A., Zhao J. *et al*.: ApcD is necessary for efficient energy transfer from phycobilisomes to photosystem I and helps to prevent photoinhibition in the cyanobacterium *Synechococcus* sp. PCC 7002. – Biochim. Biophys. Acta. **1787**: 1122-1128, 2009.

Gan F., Bryant D.A.: Adaptive and acclimative responses of cyanobacteria to far-red light. – Environ. Microbiol. **17**: 3450-3465, 2015.

Gan F., Shen G., Bryant D.A.: Occurrence of far-red light photoacclimation (FaRLiP) in diverse cyanobacteria. – Life **5**: 4-24, 2014b.

Gan F., Zhang S., Rockwell N.C. *et al*.: Extensive remodeling of a cyanobacterial photosynthetic apparatus in far-red light. – Science **345**: 1312-1317, 2014a.

Glazer A.N.: Phycobilisome a macromolecular complex optimized for light energy transfer. – BBA-Bioenergetics **768**: 29-51, 1984.

Glazer A.N.: Light guides. – J. Biol. Chem. **264**: 1-4, 1989.

Gómez-Lojero C., Pérez-Gómez B., Krogmann D.W. *et al*.: The tricylindrical core of the phycobilisome *Arthrospira (Spirulina) maxima*. – Int. J. Biochem. Cell. B. **29**: 959-970, 1997.

Gómez-Lojero C., Pérez-Gómez B., Shen G. *et al*.: Interaction of ferredoxin:NADP$^+$ oxidoreductase with phycobilisomes and phycobilisome substructures of the cyanobacterium *Synechococcus* sp. Strain PCC 7002. – Biochemistry **42**: 13800-13811, 2003.

Grossman A.R.: A molecular understanding of complementary chromatic adaptation. – Photosynth. Res. **76**: 207-215, 2003.

Guglielmi G., Cohen-Bazire G., Bryant D.A.: The structure of *Gloeobacter violaceus* and its phycobilisome. – Arch. Microbiol. **129**: 181-189, 1981.

Ho M.Y., Gan F., Shen G., Bryant D.A.: Far-red light photoacclimation (FaRLiP) in *Synechococcus* sp. PCC 7335. II. Characterization of phycobiliproteins produced during acclimation to far-red light. – Photosynth. Res. **131**: 187-202, 2017.

Ho M.Y., Shen G., Canniffe D.P. *et al*.: Light-dependent Chl *f* synthase is a highly divergent paralog of PsbA of photosystem II. – Science **353**: 886, 2016.

Houmard J., Capuano V., Colombano M.V. *et al*.: Molecular characterization of the terminal energy acceptor of cyanobacterial phycobilisomes. – P. Natl. Acad. Sci. USA **87**: 2152-2156, 1990.

Hu Q., Marquardt J., Iwasaki I. *et al.*: Molecular structure, localization and function of biliproteins in the chlorophyll *a/d* containing oxygenic photosynthetic procaryote *Acaryochloris*

marina. – Biochim Biophys Acta **1412**: 250-261, 1999.

Itoh S., Ohno T., Noji T. *et al*.: Harvesting far-red light by chl *f* in photosystems I and II of unicellular cyanobacterium strain KC1. – Plant Cell Physiol. **56**: 2024-2034, 2015.

Jordan P., Fromme P., Witt H.T. *et al*.: Three-dimensional structure of cyanobacterial photosystem I at 2.5 A resolution. – Nature **411**: 909-917, 2001.

Kehoe D.M., Gutu A.: Responding to color: the regulation of complementary chromatic adaptation. – Annu. Rev. Plant Biol. **57**: 127-150, 2006.

Li Y., Scales N., Blakenship R.E. *et al*.: Extinction coefficient for red-shifted Chls: Chl *d* and Chl *f*. – BBA-Bioenergetics **1817**: 1292-1298, 2012.

Li Y., Lin Y., Loughlin P.C., Chen M.: Optimization and effects of different culture conditions on growth of *Halomicronema hongdechloris* a filamentous cyanobacterium containing Chl *f*. – Front. Plant Sci. **5**: 67, 2014.

Li Y., Lin Y., Garvey C.J. *et al*.: Characterization of red-shifted phycobilisomes isolated from the Chl *f*–containing cyanobacterium *Halomicronema hongdechloris*. – Biochim. Biophys. Acta **1857**: 107-114, 2016.

Liu H., Zhang H., Niedzwiedzki D.M. *et al.*: Phycobilisomes supply excitations to both photosystems in a megacomplexes in cyanobacteria. – Science **342**: 1104-1107, 2013.

Loughlin P., Lin Y., Chen M.: Chlorophyl *d* and *Acaryochloris marina*: current status. – Photosynth. Res. **116**: 277-293, 2013.

Lundell D.J., Yamanaka G., Glazer A.N.: A terminal energy acceptor of the phycobilisome: the 75,000-dalton polypeptide of *Synechococcus* 6301 phycobilisome a new biliprotein. – J. Cell Biol. **91**: 315-319, 1981.

Mendoza-Hernández G., Pérez-Gómez B., Krogmann D.W. *et al*.: Interaction of linker proteins with the phycobiliproteins in the phycobilisome substructures of *Gloeobacter violaceus.* – Photosynth. Res. **106**: 247-261, 2010.

Mielke S., Kiang N., Blankenship R. *et al*.: Efficiency of photosynthesis in a Chl *d*- utilizing oxygenic species. – Biochim. Biophys. Acta **1807**: 1231-1236, 2011.

Mielke S.P. Kiang N.Y., Blankenship R.E., Mauzerall D.: Photosystem trap energies and spectrally-dependent energy storage efficiencies in the chl d-utilizing cyanobacterium, *Acaryochloris marina.* – BBA-Bioenergetics **1827**: 255-265, 2013.

Mimuro M., Lipschultz C.A., Gantt E.: Energy flow in the phycobilisome core of *Nostoc* sp. (MAC): two independent terminal pigment. – BBA-Bioenergetics **852**: 307-319, 1986.

Moore L.R., Goericke R., Chisholm S.W.: Comparative physiology of *Synechococcus* and *Prochlorococcus*: influence of light and temperature on growth, pigments, fluorescence and absorptive properties. – Mar. Ecol. Prog. Ser. **116**: 250-275, 1995.

Pérez-Gómez B., Mendoza-Hernández G., Cabellos-Avelar T. *et al*.: A proteomic approach to the analysis of the components of the phycobilisomes from two cyanobacteria with complementary chromatic adaptation: *Fremyella diplosiphon* UTEX B590 and *Tolypothrix* PCC 7601. – Photosynth. Res. **114**: 43-58, 2012.

Perkerson III R.B., Johansen J.R., Kovácik L. *et al*.: A unique Pseudanabaenalean (cyanobacteria) genus *Nodosilinean* gen. nov. based on morphological and molecular data. – J. Phycol. **47**: 1397-1412, 2011.

Reuter W., Wehrmeyer W.: Core structure in *Mastigocladus laminosus* phycobilisomes: II the central part of the tricylindrical core – AP_{CM} – contain the anchor polypeptide and no allophycocyanin B. – Arch. Microbiol. **153**: 111-117, 1990.

Schägger H., von Jagow G.: Tricine-sodium dodecyl sulfate-polyacrylamide gel electrophoresis for the separation of proteins in the range from 1 to 100 kDa. – Anal. Biochem. **166**: 368-379, 1987.

Sidler W.A. Phycobilisome a phycobiliprotein Structures. – In: Bryant D.A. (ed.): The Molecular Biology of Cyanobacteria. Pp. 139-216. Kluwer Academic Publishers, Dordrecht 1994.

Schluchter W.M., Bryant D.A.: Molecular characterization of ferredoxin $NADP^+$ oxidoreductase in cyanobacteria: cloning and sequence of the *pet*H gene of *Synechococcus* sp. PCC 7002 and studies in the gene product. – Biochemistry **31**: 3092-3102, 1992.

Souza V., Eguiarte L.E., Siefert J., Elser J.: Microbial endemism: does phosphorus limitation enhance speciation? – Nat. Rev. Microbiol. **6**: 559-564, 2008.

Souza V., Siefert J.L., Escalante A.E. *et al*.: The Cuatrociénegas Basin in Coahuila, México: An astrobiologial precambrian park. – Astrobiology **12**: 641-647, 2012.

Stackebrandt E., Goebel B.M.: Taxonomic note: a place for DNA-DNA reassociation and 16S rRNA sequence analysis in the present species definition in bacteriology. – Int. J. Syst. Bacteriol. **44**: 846-849, 1994.

Stanier G. (Cohen-Bazire): Fine structure of cyanobacteria. – Methods Enzymol. **167**: 157-172, 1988.

Stevens Jr S.E., Pat Patterson C.O., Myers J.: The production of hydrogen peroxide by blue-green algae: A survey. – J. Phycol. **9**: 427-430, 1973.

Tandeau de Marsac N., Houmard J.: Complementary chromatic adaptation: Physiological conditions and action spectra. – Methods Enzymol. **167**: 318-328, 1988.

Taton A., Grubisic S., Brambilla E. *et al*.: Cyanobacterial diversity in natural and artificial microbial mat of Lake Fryxell (Mc Murdo Dry Valleys Antarctica): A morphological and molecular approach. – Appl. Environ. Microbiol. **69**: 5157-5169, 2003.

Umena Y., Kawakami K., Shen J.R., Kamiya N.: Crystal structure of oxygen evolving photosystem II at a resolution of 1.2 A. – Nature **473**: 55-60, 2011.

Wittig I., Karas M., Schägger H.: High resolution clear native electrophoresis for In-gel functional assays and fluorescence studies of membrane protein complexes. – Mol. Cell. Proteomics **6**: 1215-1225, 2007.

Yamanaka G., Glazer A.N., Williams R.C.: Cyanobacterial phycobilisomes. Characterization of the phycobilisomes of *Synechococcus* sp. 6301. – J. Biol. Chem. **253**: 8303-8310, 1978.

Zhang Z., Schwartz S., Wagner L., Miller W.: A greedy algorithm for aligning DNA sequences. – J. Comput. Biol. **7**: 203-214, 2000.

Zuker M.: Mfold web server for nucleic acid folding and hybridization prediction. – Nucleic Acids Res. 31: 3406-3415, 2003.